2012

Actuating individual electrospun hydrogel nanofibres

Adrian Gestos
University of Wollongong, gestos@uow.edu.au

Philip G. Whitten
University of Wollongong, whitten@uow.edu.au

Gordon G. Wallace
University of Wollongong, gwallace@uow.edu.au

Geoffrey Maxwell Spinks
University of Wollongong, gspinks@uow.edu.au

Publication Details

Gestos, A, Whitten, PG, Wallace, GG & Spinks, GM (2012), Actuating individual electrospun hydrogel nanofibres, Soft Matter, 8(31), pp. 8082-8087.

Actuating individual electrospun hydrogel nanofibres

Abstract
The actuation of a single hydrogel nanofibre is measured for the first time by AFM. The actuation stress generated was comparable to that produced by skeletal muscle and the actuation rate was significantly increased by the nanoscale dimensions of the fibre.

Keywords
electrospun, hydrogel, individual, actuating, nanofibres

Publication Details
Gestos, A, Whitten, PG, Wallace, GG & Spinks, GM (2012), Actuating individual electrospun hydrogel nanofibres, Soft Matter, 8(31), pp. 8082-8087.

Soft Matter

Cite this: *Soft Matter*, 2012, **8**, 8082

www.rsc.org/softmatter

PAPER

Actuating individual electrospun hydrogel nanofibres†

Adrian Gestos, Philip G. Whitten, Gordon G. Wallace and Geoffrey M. Spinks*

Received 20th February 2012, Accepted 25th April 2012
DOI: 10.1039/c2sm25387a

The actuation of a single hydrogel nanofibre is measured for the first time by AFM. The actuation stress generated was comparable to that produced by skeletal muscle and the actuation rate was significantly increased by the nanoscale dimensions of the fibre.

Introduction

Hydrogels have long been proposed and investigated as artificial muscle materials,[1] but few real applications have emerged to date. The principal problem with hydrogel actuators is their prohibitively slow actuation rate. Hydrogel volume transitions triggered by changes in temperature, pH and ionic strength involve the mass transport of solvent (water) into and out of the hydrogel.[2] The water diffusion coefficient in hydrogels[3] is typically 1–10 $\mu m^2\ s^{-1}$ so that the equilibrium swelling time for millimetre scale gels can be several hours.[4–6] Diffusion time is inversely proportional to the square of the diffusion distance[3,7] and rapid swelling transitions have been shown to occur in micro- and nano-gel structures[8,9] and in porous gels.[4,10]

Hydrogel micro- and nano-fibres are particularly promising for artificial muscles. Most attention has been given to hydrolysed polyacrylonitrile (PAN) gel fibres since they can be prepared from commercially-available PAN by treatment with a strong base.[11] Samples are typically hundreds of fibres bundled together with individual filament diameters in the tens of micrometres. Actuation strains of 20–100% have been achieved by changing the pH of the surrounding solution[12] with response times of 5–10 s.[11,13] Attempts to reduce the response time by preparing bundles of PAN nanofibres (700 nm diameter) have to date been unsuccessful,[14] perhaps due to the slow infusion of pH solution inside the bundle. Actuation in single hydrogel nanofibres has recently been directly observed using atomic force microscopy[15,16] although no attempt was made to measure actuation speed.

Investigating the fundamental actuation performance of individual nano-fibre hydrogels is challenging because of their softness and fragility. The recent advent of a range of new tough hydrogels[17] offers the prospect of forming thin films and fibres that are sufficiently robust for actuation testing. It is especially important to characterise the actuation performance with an external stress applied to the actuator material,[18] since it is known that the pH-induced actuation strain of hydrogel microfibre bundles decreases with an increase in applied external stress.[13,19] For thin hydrogel fibres, the maximum external loads must be small: a fibre of 500nm diameter with a Young's modulus of 50 kPa requires a force of only 1 nN for a 10% strain. Recently, a method using an atomic force microscope (AFM) has been described that allows tensile testing of individual nanofibres to high strains with sub nN force resolution.[20,21] The method is applicable to soft, elastomeric materials and allows the samples to be immersed in a fluid. The technique is ideally suited for actuation testing of individual hydrogel nanofibres.

The current study evaluates the pH-induced actuation performance of individual hydrogel nanofibres. Of particular interest was the determination of the rate of response to a pH change and the evaluation of the effect of an applied external stress on the actuation. The latter is likely to be significant for hydrogels since the Young's modulus is known to change during the volume transition[22–24] and will, therefore, produce a change in strain in proportion to the applied external stress.[18] The modulus-induced strain has been little studied in hydrogel materials[25] and the new AFM tensile testing method allows this phenomenon to be investigated in individual hydrogel nanofibres for the first time.

Methods

Reagents and materials

Buffers of pH 3 and pH 8 were prepared by mixing different ratios of 0.1 M citric acid (Sigma-Aldrich) and 0.2 M disodium hydrogen phosphate heptahydrate (Fluka).[26] Poly(acrylic acid) (PAA) (M_w ~450,000 g mol^{-1}) was purchased from Polysciences, Inc. All chemicals were used as received. Aqueous solutions were prepared using Milli-Q water (resistivity of 18.2 MΩ cm). 3-aminopropyltriethoxysilane (APTES) was purchased from Gelest. The UV-curable glue was purchased from DYMAX (425:light weld).

Amine functionalisation of AFM cantilevers

AFM cantilevers were amine-functionalised with APTES to increase their adhesion to the hydrogel PAA electrospun fibres

ARC Centre of Excellence for Electromaterials Science, Intelligent Polymer Research Institute, AIIM Facility, Innovation Campus University of Wollongong, NSW 2522, Australia. E-mail: geoff_spinks@uow.edu.au; Fax: +61 2 42213114; Tel: +61 2 42213010

† Electronic Supplementary Information (ESI) available. See DOI: 10.1039/c2sm25387a/

and prevent slippage during testing. The functionalisation was achieved by initially treating the cantilever for 10 min in a commercial ultra-violet/ozone (UVO) cleaner (Jelight Company Inc. 42-220), followed by soaking in a 3% v/v aqueous solution of APTES for 5 min. The cantilever was then rinsed with fresh acetone and blown dry under a stream of nitrogen gas.

Fabrication of electrospun and crosslinked fibres for actuation testing

PAA was electrospun from a blunt, cylindrical syringe tip with an internal diameter of 150 μm (Dispense Tips, Nordson EFD). Using a high voltage power supply, (Gamma High Voltage ES-30) a voltage of 10 kV was applied to an aqueous solution of 8% w/v PAA dispensed at a flow rate of 0.2 ml h^{-1} using a syringe pump (KD Scientific, KDS 100). The separation between syringe tip and collector was 180 mm and a low humidity atmosphere was maintained by a flow of dry nitrogen gas into the closed electrospinning chamber.

As reported previously,[20] it is preferable to suspend the nanofibres across a trench for AFM tensile testing in lateral (horizontal) AFM mode. This testing configuration was easily achieved by electrospinning the fibres directly onto supporting grids normally used for transmission electron microscopy (TEM). The TEM grids had parallel bars (Gold, Gilder Grids) of 40 μm width separated by 50 μm gaps and were attached to glass slides for ease of handling. The TEM grids formed the collector for electrospinning and were configured as described by Shin *et al.*[27] such that fibres were aligned and deposited perpendicular to the bars of the TEM grid.

The PAA electrospun nanofibres were crosslinked by exposure to UVC radiation for 5 min under a nitrogen atmosphere (denoted as UVN_2) within a UVO cleaner as described previously.[16] After crosslinking, the fibres were pinned in place on the bars of the TEM grid with UV-curable glue which was applied with a glass microfibre, positioned with a micromanipulator, (Marzhauser Wetzlar DC-3 K) while being observed under an optical microscope. Along the length of the fibre, some portions were left uncovered by glue to allow for imaging with the AFM to determine the fibre cross-sectional area.

Actuation measurements

Actuation performance was determined by measuring the change in tensile force in stretched nanofibres when the pH of the surrounding solution was changed. The fibres were stretched by lateral movement of the fully-immersed AFM cantilever, using the method similar to that described previously[20,21] and illustrated in Fig. 1a. The fibre was initially immersed in pH ~3 solution and stretched at its midpoint to a strain that was sufficient for the fibre to remain under tension once it was eventually swollen at pH 8. The pH was then cycled from pH ~3 to pH ~8, followed by a pause, then back again to pH ~3. Changes in pH were affected by infusing ~30 ml of the appropriate solution through the petri dish (total volume of 10 ml) with a push/pull syringe pump operating at 3.5 ml min^{-1}. At each pH the fibre was also subjected to a small amplitude strain cycle to determine the elastic modulus. The cantilever was scanned back and forth over 500 nm (equivalent to a strain of approximately 1%) at a constant

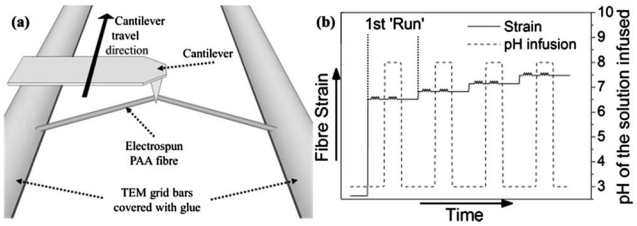

Fig. 1 (a) diagram of actuation testing apparatus; (b) schematic illustration of the procedure for carrying out constant strain actuation measurements at increasing strains. Each "run" consisted of an initial pre-strain adjustment at pH 3 followed by a small amplitude strain oscillation to determine modulus after which the pH was changed to pH 8 and the small amplitude strain oscillation repeated.

500 nm s^{-1} for a minimum of 5 cycles. Once the pH had been cycled and the 500 nm scans carried out, the fibre strain was then incrementally increased by ~2.5%. The pH cycling and 500 nm cantilever scans were then repeated in the same manner at each strain increment. For ease of expression, this procedure (pH cycling and 500 nm scans) carried out at a single strain will be referred to as a 'run' and is schematically illustrated in Fig. 1b.

The lateral twist of an AFM cantilever was used as the force sensor for the actuation measurements. The calibration of the cantilever force to lateral deflection ratio (N/V_l), or 'lateral force conversion factor' (α_l), was determined by the use of a glass fibre as a reference beam.[28] The fibres are assumed to undergo purely axial tensile stretching rather than bending during the three point mechanical test used here as is known to occur with low Young's modulus ($\ll$10 GPa) fibres of high aspect ratio of length to width (>30 : 1).[29–31]

Results and discussion

Free swelling of individual nanofibres

Microscopic observation of tethered PAA nanofibres during a change of solution pH showed large and rapid actuation. The fibres were fixed to the bars of a TEM grid and immersed in pH ~3 solution, but were not contacted by the AFM cantilever. Fast infusion of pH ~ 8 buffer at a rate of ~5 ml s^{-1} caused rapid swelling of the fibres generating an axial strain of 15–19% (Fig. 2). De-protonation of the carboxylic acid at pH above ~5 causes swelling of the PAA from the increased osmotic pressure and charge repulsion resulting from the negatively charged

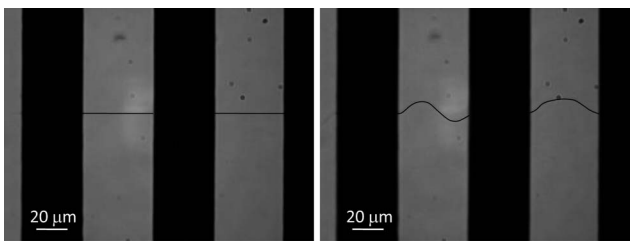

Fig. 2 Still images from a video taken through an optical microscope of PAA nanofibres UVN_2 treated for 5 min and suspended between the bars of a TEM grid (left) contracted at pH ~3 and (right) swollen at pH ~8. The fibres are traced with a black line for clarity as they are faint in the unaltered picture.

carboxylate groups. Evaluation of the video images gives an estimated response time of 1–4 s (see video in ESI†), although accurate determination was difficult since the fibres moved outside the focal plane of the microscope. Given a water diffusion coefficient at the lower end of the range typical for hydrogels of ~1 $\mu m^2\ s^{-1}$, the expected response time for these nanofibres (730 nm diameter in the fully swollen state) would be ~10 msec based on the diffusion kinetics described by Shibayama and Tanaka.[32] The slower than expected response of the PAA nanofibres may be due to slow solution mixing, rate-limiting acid–base reactions or non-typical diffusion processes. Similarly slow response of hydrogel microfibers has also been reported previously[33] and is the subject of on-going investigations.

Actuation of stretched nanofibres

The actuation response with an applied external load was also determined using the AFM system with the fibres held at constant strain. It was found that the infusion of pH solution into the testing cell caused a temporary disturbance to the AFM lateral force signal even when a nanofibre sample was not present (Fig. 3). As such, it was only possible to determine the overall actuation force change caused by the nanofibre expansion/contraction (Fig. 3), and the transient force responses were ignored (dashed lines in Fig. 4). The transition time was slightly longer for the pH 3 infusion compared to the pH 8 infusion, since a larger volume of buffer was required to alter the pH in the former case.

The sequence of force changes acting on the fibre (F_t) over a single run is illustrated in Fig. 4. The point of 0 s was taken where the initial pre-strain of 30% was first applied to the fibre in a pH 3 solution. The F_t initially decreased to a small degree after the initial application of strain to the fibre, due to viscoelastic relaxation. Once the F_t stabilised (~50 s), a series of lateral tip oscillations (500 nm scans) were applied to the fibre to determine the stiffness and elastic modulus (E). The infusion of pH 8 solution was commenced at ~100 s. A slow infusion rate of 3.5 ml min^{-1} was used to minimise the temporary disturbance to the AFM signal, but also resulted in an apparently slower actuation response than observed in the free-swelling experiments. The decrease in the measured force acting on the fibre at fixed strain was due to an increase in the fibre length. Once the fibre had stopped swelling and F_t stabilised (~240 s) a second series of tip oscillations was performed to determine the fibre stiffness and modulus at pH ~8. The testing sequence was then concluded by infusion of the pH 3 solution (~320 s) leading to an increase in F_t. Here, the increase in F_t was caused by the polymer chains behaving as entropic springs, which is associated with fibre shrinkage due to the pH dropping below pH 5. Once the F_t had again stabilised (~600 s), the fibre pre-strain was increased and the next run commenced.

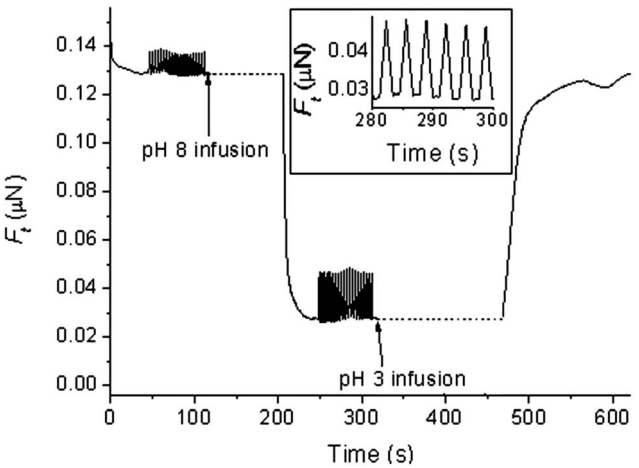

Fig. 4 F_t *versus* time for the same run with a fibre attached that is presented in Fig. 3 and inset showing an expanded portion of the graph that more clearly displays the additional 500 nm cantilever scans. The dashed lines represent where the drift in force due to pH solution mixing was removed from the data.

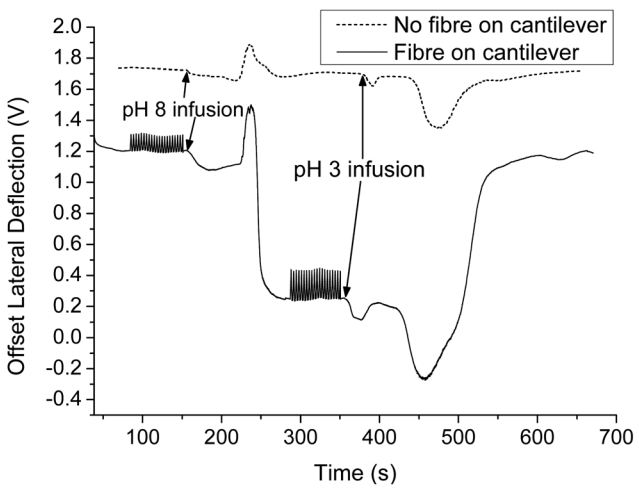

Fig. 3 Lateral deflection *versus* time raw data obtained during a single run with and without a PAA fibre attached and stretched by the cantilever. Where the cantilever is attached to a fibre, the fibre is stretched to a strain of 30%. The arrows indicate the starting time of the relevant pH solution infusion.

The mechanical parameters associated with pH induced change in tension force in the nanofibres are illustrated in Fig. 5. The initial setup involves applying a fixed pre-strain to the nanofibre at pH ~3 with the polymer in the less-swollen, protonated form. The change in pH induces a change in fibre

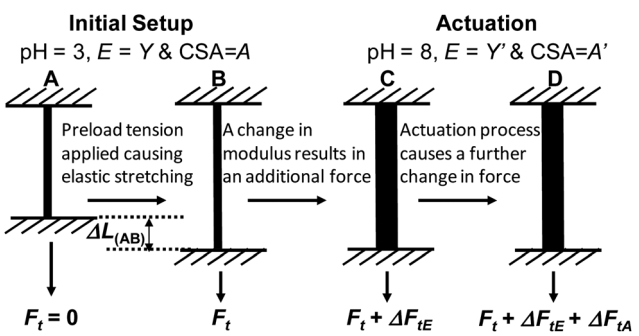

Fig. 5 Illustration of the PAA fibre held at a constant strain and the components that make up the total force acting on the fibre (F_t) upon swelling at pH 8, adapted from.[34] Young's modulus (E) and fibre cross-sectional area (CSA) are also noted.

cross-sectional area (A) and modulus (E) contributing to the measured change in tensile force. The actuation measurements consider the force change occurring from steps B to D ($F_{t(\mathrm{BD})}$) as shown in Fig. 5, which are classified as isometric (constant length) actuation.

The $F_{t(\mathrm{BD})}$ change occurring in the PAA nanofibre due to the pH shift from 3 to 8 was modelled by the following linear-elastic equation:[18,34]

$$F_{t(\mathrm{BD})} = \frac{\Delta L_{(\mathrm{AB})}}{L_0}(A'Y' - AY) - \frac{\Delta L_0}{L_0}A'Y' \quad (1)$$

where $\Delta L_{(\mathrm{AB})}$ is the initial pre-stretch applied at pH 3 (the pre-strain is $\varepsilon_{(\mathrm{AB})} = \Delta L_{(\mathrm{AB})}/L_0$); L_0 is the initial length at pH 3 prior to stretching; A and Y are, respectively, the cross-sectional area and Young's modulus at pH 3; A' and Y' are, respectively, the cross sectional area and Young's modulus at pH 8 and ΔL_0 is the free stroke or the change in length expected at zero applied stretch due to a change in pH from 3 to 8. Eqn (1) is based on the assumption that the nanofibres are linearly elastic materials, which is approximately true over the strain range of ~28% to ~40% used in the actuation tests (Fig. 6). From eqn (1) it is expected that a plot of $F_{t(\mathrm{BD})}$ obtained at each pre-strain should be linear, with:

$$Slope = \frac{1}{L_0}(A'Y' - AY) \quad (2)$$

$$Intercept = \frac{-\Delta L_0}{L_0}A'Y' \quad (3)$$

The stiffness (S at pH 3, S' at pH 8) of the fibres measured during the 500 nm tip oscillation scans at each pH is:

$$S = \frac{\delta f}{\delta L} = \frac{AY}{L_0} \quad (4)$$

and by rearranging eqn (2) then substituting from eqn (4) to obtain:

$$Slope = \left(\frac{A'Y'}{L_0} - \frac{AY}{L_0}\right) = (S' - S) \quad (5)$$

The plot of $F_{t(\mathrm{BD})}$ *versus* $\Delta L_{(\mathrm{AB})}$ for three separate fibres is presented in Fig. 7 along with the tabulated data of the experimentally and theoretically determined actuation parameters in Table 1. The experimentally measured force changes are all negative, since the tension force decreases as the nanofibre swells with an increase in the pH from 3 to 8. For each of the three nanofibres tested there is a clear decrease in the magnitude of the force change ($F_{t(\mathrm{BD})}$) that occurs during actuation when the extent of static pre-stretch ($\Delta L_{(\mathrm{AB})}$) was increased. That is, the further the fibre was stretched at pH 3, the smaller was the force change when the pH was increased to 8. There were some differences observed in the force changes measured for each fibre at a given pre-stretch degree, however, the difference was within the previously reported experimental error of 26%[28] observed for lateral force cantilever calibration.

The decrease in the magnitude of force change in response to higher pre-strains indicates that the nanofibres increase in stiffness as they swell. That is, the decrease in holding force due to fibre swelling is partially offset by an increase in stiffness, with the force generated by the latter proportional to the initially applied pre-strain. The dashed lines shown in Fig. 7 are least-squares linear fits to the experimental data highlighting the linear dependence of the force change with the amount of pre-stretch and in agreement with eqn (1). Further, the slopes of the linear fits correlate closely to the difference in nanofibre stiffness (S'-S) as measured experimentally and as expected from eqn (5). Estimation of the Young's modulus from the measured stiffness and the cross-sectional area (Table 1) show that the increased stiffness at pH 8 compared to pH 3 is due to the larger cross-sectional area in the swollen state. The Young's modulus actually decreases as the PAA swells at pH 8.

The Young's modulus values are significantly higher than is typical of high-swelling hydrogels and is due to the relatively low water content of these crosslinked PAA nanofibres. There is a strong correlation between the Young's moduli of hydrogels and their swelling degree in water. Hydrogels with swelling ratios

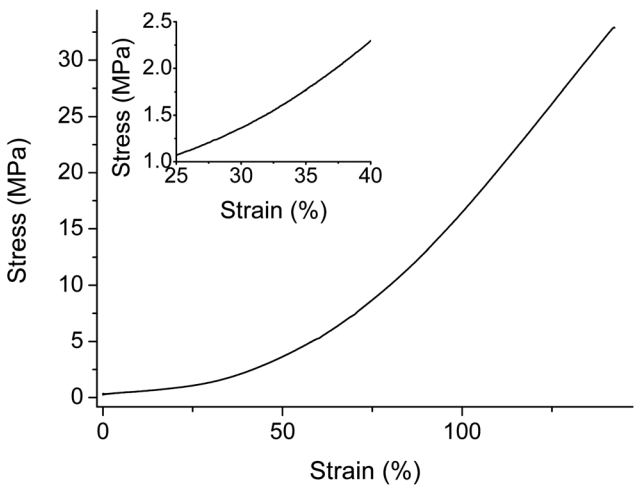

Fig. 6 A representative stress-strain curve of a PAA nanofibre in solution at pH 3 with inset showing a close up of the strain range covered by the $\Delta L_{(\mathrm{AB})}$ used in the actuation tests.

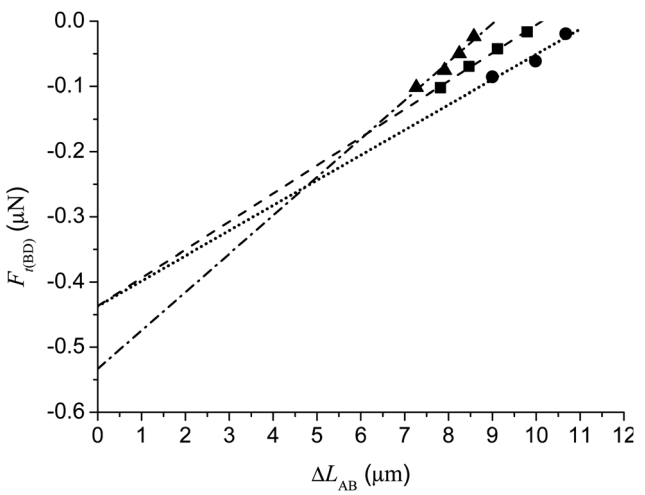

Fig. 7 Force generated ($F_{t(\mathrm{BD})}$) by the three PAA fibres measured at different initial pre-stretch (ΔL_{AB}).

Table 1 Properties of the three fibres tested, those denoted with and without an apostrophe represent respectively, pH 8 and pH 3 conditions

	Stiffness (N m^{-1})				Area (μm^2)		Modulus (MPa)		Calculated free stroke	
Fibre	S	S'	S'-S	Slope[a] (N m^{-1})	A	A'	Y	Y'	ΔL_0 (μm)	ε_0 (%)
1	0.040	0.080	0.040	0.043	0.12	0.42	9.3	5.2	5.5	20
2	0.047	0.097	0.050	0.059	0.12	0.42	9.7	5.5	5.5	23
3	0.026	0.064	0.038	0.039	0.12	0.42	6.6	4.5	6.8	24

[a] Obtained from Fig. 7.

of fully swollen mass to dry mass in the range of 10–30 typically have moduli in the range 0.1–0.01 MPa, while hydrophobically modified hydrogels with lower swelling ratios (2–10) have moduli of 0.1–10 MPa.[17] Previous studies of PAA nanofibres prepared identically to those used in the present study have a swelling ratio of 2 (pH 3) to 7 (pH 8), and this low swelling degree at least partially accounts for their high moduli. Electrospun nanofibres are also known to be highly aligned and the axial alignment of the polymer chains also contributes to a higher modulus.[27,35,36]

Extrapolation of the experimental data in Fig. 7 to zero pre-stretch gives an intercept value that can be used to determine the free stroke resulting from a change in pH from 3 to 8. These calculated free strains are in the range of 20–24% for the three PAA nanofibres (Table 1). These values are slightly higher than those experimentally estimated from the video analysis of the free actuation (15–19%). The latter values are likely to underestimate the true value due to some of the fibre's length not being parallel to the viewable plane in the microscope image. Within these experimental uncertainties, the two measurements of the free strain are taken to be equivalent.

The PAA nanofibres measured here can be compared to previously reported hydrogels in terms of their practical application. The maximum force generated (at zero pre-stretch) is of the order of 0.4 μN corresponding to a stress of 230 kPa, which is significantly larger than measured for single PAN filaments (44 kPa)[13] and similar to that produced by skeletal muscle (300 kPa).[37]

Conclusions

The pH-induced actuation force generated by individual PAA nanofibres when held at increasing constant pre-strains was measured successfully for the first time. An AFM-based system was used to pre-stretch the fibres and measure the force changes with high sensitivity. The actuation stress generated was similar in magnitude to that produced by skeletal muscle (~300 kPa). The actuation force decreased in magnitude when a higher pre-strain was applied. This effect was due to the increase in stiffness of the fibre that occurs simultaneously with the fibre swelling. This behaviour was satisfactorily explained by a simple linear model previously developed for bulk scale conducting polymer actuators.[18] As a result, the measured actuation force could be predicted from the free stroke, cross-sectional area and stiffness of the nanofibre. Direct observations showed the free strain to be ~20% and the strain rate to be up to 20%/s demonstrating the advantage of nanofibres for fast actuation.

Acknowledgements

The authors thank the Australian Research Council (ARC) for financial support, and the ANFF Materials Node for their provision of research facilities. G.M.S. and G.G.W. were supported by ARC Professorial Fellowship and ARC Federation Fellowship, respectively. The authors are also grateful to Dr Michael Higgins for useful discussions.

Notes and references

1 P. Calvert, *"Polymer Gel Actuators: Fundamentals," in Biomedical Applications of Electroactive Polymer Actuators*, ed. F. Carpi and E. Smela, John Wiley & Sons, 2009.
2 R. M. Ottenbrite, K. Park, and T. Okano, *Biomedical applications of hydrogels handbook*. New York, Springer Verlag, 2010.
3 T. Tanaka and D. J. Fillmore, *J. Chem. Phys.*, 1979, **70**, 1214.
4 J. T. Zhang, R. Bhat and K. D. Jandt, *Acta Biomaterialia*, 2009, **5**, 488.
5 K. A. George, E. Wentrup-Byrne, D. J. T. Hill and A. K. Whittaker, *Biomacromolecules*, 2004, **5**, 1194.
6 B. Adnadjevic and J. Jovanovic, *J. Appl. Polym. Sci.*, 2008, **107**, 3579.
7 E. Sato Matsuo and T. Tanaka, *J. Chem. Phys.*, 1988, **89**, 1695.
8 J. Wang, A. Sutti, X. Wang and T. Lin, *Soft Matter*, 2011, **7**, 4364.
9 Y. Tan, K. Xu, P. Wang, W. Li, S. Sun and L. Dong, *Soft Matter*, 2010, **6**, 1467.
10 J. Chen and K. Park, *Carbohydr. Polym.*, 2000, **41**, 259–268.
11 D. Brock, W. Lee, D. Segalman and W. Witkowski, *J. Intell. Mater. Syst. Struct.*, 1994, **5**, 764–771.
12 K. Choe and K. J. Kim, *Sens. Actuators, A*, 2006, **126**, 165.
13 K. Choe, K. J. Kim, D. Kim, C. Manford, S. Heo and M. Shahinpoor, *J. Intell. Mater. Syst. Struct.*, 2006, **17**, 563–576.
14 D. Y. Lee, Y. Kim, S. Lee, M. Lee, J. Lee, B. Kim and N. Cho, *Mater. Sci. Eng., C*, 2008, **28**, 294.
15 R. Samatham, I.-S. Park, K. J. Kim, J.-D. Nam, N. Whisman and J. Adams, *Smart Mater. Struct.*, 2006, **15**, N152.
16 A. Gestos, P. G. Whitten, G. M. Spinks and G. G. Wallace, *Soft Matter*, 2010, **6**, 1045.
17 S. Naficy, H. R. Brown, J. M. Razal, G. M. Spinks and P. G. Whitten, *Aust. J. Chem.*, 2011, **64**, 1007.
18 G. Spinks and V. Truong, *Sens. Actuators, A*, 2005, **119**, 455.
19 L. Yu and L. Gu, *Eur. Polym. J.*, 2009, **45**, 1706.
20 A. Gestos, P. G. Whitten, G. M. Spinks and G. G. Wallace, To be submitted.
21 C. R. Carlisle, C. Coulais, M. Namboothiry, D. L. Carroll, R. R. Hantgan and M. Guthold, *Biomaterials*, 2009, **30**, 1205.
22 K. S. Anseth, C. N. Bowman and L. Brannon-Peppas, *Biomaterials*, 1996, **17**, 1647.
23 R. Skouri, F. Schosseler, J. P. Munch and S. J. Candau, *Macromolecules*, 1995, **28**, 197.
24 M. Rubinstein, R. H. Colby, A. V. Dobrynin and J.-F. Joanny, *Macromolecules*, 1996, **29**, 398.
25 S. J. Kim, G. M. Spinks, S. Prosser, P. G. Whitten, G. G. Wallace and S. I. Kim, *Nat. Mater.*, 2006, **5**, 48.
26 T. A. McIlvaine, *Journal of Biological Chemistry*, 1921, **49**, 183.
27 M. K. Shin, S. I. Kim, S. J. Kim, S.-K. Kim, H. Lee and G. M. Spinks, *Appl. Phys. Lett.*, 2006, **89**, 231929.

28 W. Liu, K. Bonin and M. Guthold, *Rev. Sci. Instrum.*, 2007, **78**, 063707.
29 D. Almecija, D. Blond, J. E. Sader, J. N. Coleman and J. J. Boland, *Carbon*, 2009, **47**, 2253.
30 D. A. Walters, L. M. Ericson, M. J. Casavant, J. Liu, D. T. Colbert, K. A. Smith and R. E. Smalley, *Appl. Phys. Lett.*, 1999, **74**, 3803.
31 Y.-J. Kim, K. Son, I.-C. Choi, I.-S. Choi, W. I. Park and J. il Jang, *Adv. Funct. Mater.*, 2011, **21**, 279.
32 M. Shibayama and T. Tanaka, *Adv. Polym. Sci.*, 1993, **109**, 1.
33 A. Sahoo, M. Jassal and A. K. Agrawal, *J. Appl. Polym. Sci.*, 2008, **109**, 3792.
34 G. M. Spinks, T. E. Campbell and G. G. Wallace, *Smart Mater. Struct.*, 2005, **14**, 406.
35 C.-L. Pai, M. C. Boyce and G. C. Rutledge, *Polymer*, 2011, **52**, 2295.
36 M. Naraghi, S. N. Arshad and I. Chasiotis, *Polymer*, 2011, **52**, 1612.
37 G. H. Pollack, F. A. Blyakhman, F. B. Reitz and O. V. Yakovenko, *"Natural Muscle as a Biological System," in Electroactive Polymer (EAP) Actuators as Artificial Muscles: Reality, Potential, and Challenges*, 2nd ed., Y. Bar-Cohen, Ed. SPIE Press Monograph.